Picosecond Laser Surface Micro/Nano Texturing of Stainless Steel as a Method to Reduce the Adhesion of Bacteria

Fatema H. RAJAB[*1], P. BENSON[2], Lin LI[1] and K. A. Whitehead[2]

[*1] *Laser Processing Research Centre, School of Mechanical, Aerospace and Civil Engineering, The University of Manchester, Manchester, M13 9PL, UK*
Fatema.rajab@postgrad.manchester.ac.uk
[2] *School of Healthcare Science, Manchester Metropolitan University, Manchester, M1 5GD, UK*

Biofilm formation and colonization is initiated by bacterial attachment followed by bacterial adhesion and retention on a surface. The buildup of biofilms may result in related health problems in the medical field and potential biofouling issues in industrial settings leading to increased economic burden. The design and manufacture surfaces that prevent bacterial attachment, retention and biofilm formation through their physical structure and chemical properties provides a potential solution to tackle such issues. Laser surface texturing provides a crucial role for the production of different antifouling surface patterns for use in a diverse range of applications in different medical or industrial fields. In the present work, a 1064 nm Nd:YVO_4 Picosecond laser was used to produce a range of textures on 316L stainless steel (SS) substrates. Results showed that the S_a values and wettability of the surfaces all increased when compared to the control following laser treatment. This work demonstrated that on all the surfaces, for all the assays, the number of adhesive bacteria on the laser textured surfaces was reduced compared to the untreated substrate. One surface was demonstrated to be the best antiadhesive surface which was of higher roughness and superhydrophobicity.

Keywords: Picosecond Laser, bacteria, superhydrophobic, roughness, biofouling

1. Introduction

Biofouling on surfaces can produce a number of economic and contamination issues in a variety of industries [1]. Bacterial attachment is the prerequisite to such fouling and is followed by bacterial adhesion and retention on a surface. The modification of a substrates topography, and or chemistry can be used to alter the microbial attachment. The effect of surface properties on bacterial attachment has been reported in many studies [2-8]. Some reported that there is a correlation between surfaces roughness and bacteria attachment and the retention of microorganisms increased with increasing the surface roughness [4-6]. However, others have reported that there is no correlation between surface roughness and bacteria attachment [7, 8]. The effect of surface wettability on bacteria attachment has also been carried out and some have been reported that the number of adhered bacteria is dramatically decreased with increasing the surface hydrophobicity and bacteria adhered to hydrophobic materials being more easily removed by an increased flow or an air-bubble jet [9-11] while others reported that there is no relationship between surface wettability and bacteria attachment [12]. In nature, there are many plants with hierarchical surface structures that are considered as self-cleaning surfaces such as lotus leaf. These surfaces are superhydrophobic with contact angles ≥ 150 ° and sliding angles < 5 ° [13]. Several studies of bacterial attachment and retention on such biomimetic type features for example the lotus leaf [9] or Taro leaf [14], have been carried out.

Different techniques such as lithography [15], moulding [16] and photolithography [17] have been used to produce different micro / nano structures. Among these techniques, laser generated micro/nano topographies are comparable for their simplicity, safety and environmentally clean and can be used for processing different substrates in different environments [18]. Laser surface modification has been extensively studied for different applications [19-21]. Stainless steel is a useful alloy in several industrial applications. This paper focuses on the production three topographies on stainless steel using picosecond laser and the effect of their altered surface properties on bacterial attachment, adhesion and retention.

2. Experimental Section

2.1 Laser Surface Texture

A 316L stainless steel substratum with a 0.7 mm thickness and 5 mm × 5 mm dimension was used in this work. Before laser treatment, the samples were cleaned ultrasonically with acetone followed by ethanol then deionized water for 10 min each. The experiment was performed using EdgeWave Nd:YVO_4 picosecond laser of (10 ps pulse duration, 103 KHz repetition rate, 1.064 µm, 125 µm beam size) in an ambient air using scanning parameters listed in (Table 1). The scanning was performed with parallel lines patterns (Fig. 1). After laser treatment, the samples were cleaned ultrasonically with ethanol then dried using compressed air to remove any ablated debris or contamination. The samples were immersed into a 1 % hetadecafluoro-

1,1,2,2-tetrahydro-decyl-1-trimethoxysilane($CF_3(CF_2)_7(CH_2)_2Si(OCH_3)_3$ (supplied by (Gilest Inc., USA)) methanol solution for 2h followed by rinsing with ethanol and drying in an oven at 80 °C for 30 min.[22].

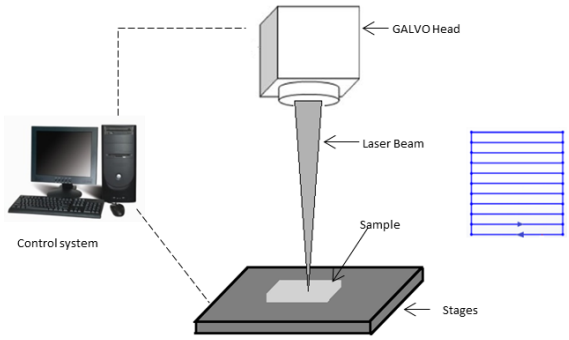

Fig. 1 Experimental set up of laser surface texturing.

Table 1 Laser processing parameters used to produce the different types of textures.

Texture	Fluence (J/cm^2)	Scanning Speed (mm/s)	Hatch distance (µm)
316 stainless steel (Control)	N/A	N/A	N/A
Hair like structures (SS1)	0.1345	1000	50
Oval wavelets in linear pattern (SS2)	0.178	100	80
Oval shaped, rounded (pillow like structure) (SS3)	0.1345	1	10

2.2 Surface Characterization

After laser treatment, the surface microtopogrophy and roughness values of the substrata were characterized using whit light interferometer (Zygo, USA). Values of S_a, S_q and S_{pv} of each surface were recorded. Selected line scans were used to determine the height, depth and width of the peaks and valleys. Atomic force microscopy Dimension 3100 (Veeco Instruments Inc., UK) was used to examine the nanotopography of the surfaces. The microstructure of the surfaces was imaged using The SEM (Philips XL30 FEG-SEM and Quanta 200x) and the EDX analysis was also carried out (Bruker energy dispersive spectroscopy analytical system).

2.3 Microbiology

One hundred milliliters of nutrient broth (Oxoid, UK) was inoculated with a single colony of Escherichia coli NCTC 9001 and incubated at 37 °C overnight. Then, cells were harvested at 3500 rpm for 10 min and were re-suspended to Optical Density (OD) 1.0 ± 0.1 at 540 nm in sterile distilled water. Serial dilutions were used to determine the colony-forming units mL^{-1} (cfu/mL) and were 2.83 x 10^9 cfu/mL. Three assays were used namely, spray with wash (Attachment), spray (Adhesion) and retention assays. Following spray with wash (Attachment) and spray (Adhesion) assays, three replicates of the textured or control surfaces were attached to a stainless steel tray using adhesive gum. Bacterial suspension (OD 1.0 @ 540 nm) was placed into the spray reservoir of a Badger Airbrush (Shesto, UK), propelled by a Letraset 600 mL liquid gas canister (Esselte Letraset Ltd, UK). The surfaces were placed vertically in a class 2 flow hood. The airbrush was sprayed over the substrate at a distance of 10 cm for 10 s. After spraying, the samples were divided into two sets, one was laid horizontally and left to dry (spray assay) and other were rinsed gently with distilled water and left to dry (spray with wash). Following retention assay, the textured surfaces as well as a control substratum (without texturing) were placed in sterile Petri dishes and 25 mL of cell suspension at OD 1.0 ±0.1 was added. The surfaces were incubated without agitation for 1h. The surfaces were washed gently and left to dry. The samples were then prepared for SEM imaging. Prior for SEM imaging, the samples were immersed in 4 % glutaraldehyde overnight at 4 °C. Samples were thoroughly rinsed with distilled water and were dried. The surfaces with retained bacteria were attached to SEM stubs with carbon tabs prior to being sputter coated with a gold and palladium coating (Model: SC7640, Polaron, Au/Pd target, deposition time: 1.5 min). SEM was carried out using a Supra 40VP with SmartSEM software (Carl Zeiss Ltd. UK). All the images were taken at 15,000 X magnification.

3. Results

3.1 Laser Surface Texturing

Three self-organized structures on stainless steel were formed using picosecond laser. SEM (Fig. 2) and white light interferometer 2D and 3D profile (Fig. 3) (Table 2) showed a range of different regular surface features at the macro/micro scale. These structures demonstrated a range of different surface features which were dependent on the laser parameters that were used. The control surface was observed to be flat with irregularly space, parallel striations of different widths and depths (Fig. 2, 3a). It demonstrated the least surface topography and the width and height of the peaks being at the lower end of the surface roughness's demonstrated (3.61 µm and 0.06 µm). It also demonstrated the lowest max valley width (1.24 µm) and in comparison with the other surfaces a fairly low max valley depth (0.09 µm). Surfaces produced using high scanning speed of 1000 mm/s (SS1) produced the least differences in surface features when compared to the controls (Fig. 2, 3b). It demonstrated regularly spaced hair like structures showed very similar topographies to the control surface. Surfaces using a hatch distance of 80 µm and scanning speed of 100 mm/s (SS2) produced a surface topography that demonstrated oval wavelets in linear patterns which had small regularly

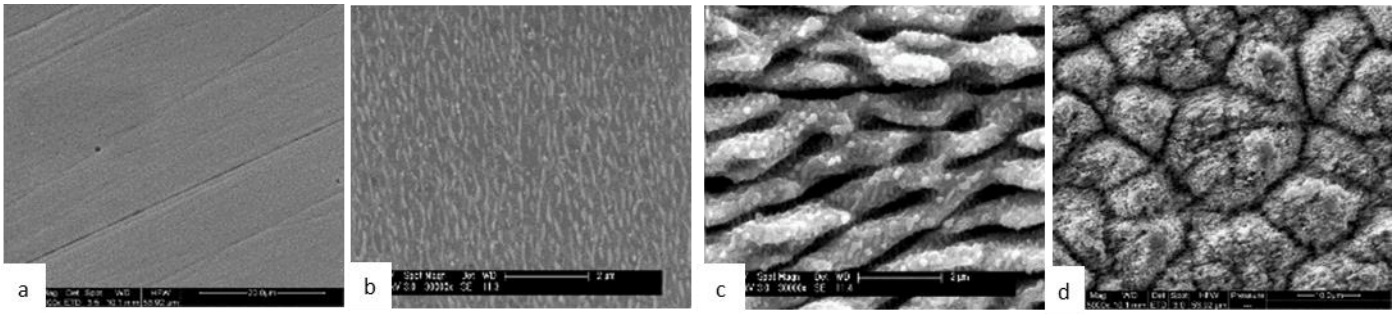

Fig. 2 SEM images of the different surface features: (a) control, (b) SS1, (c) SS2 and (d) SS3.

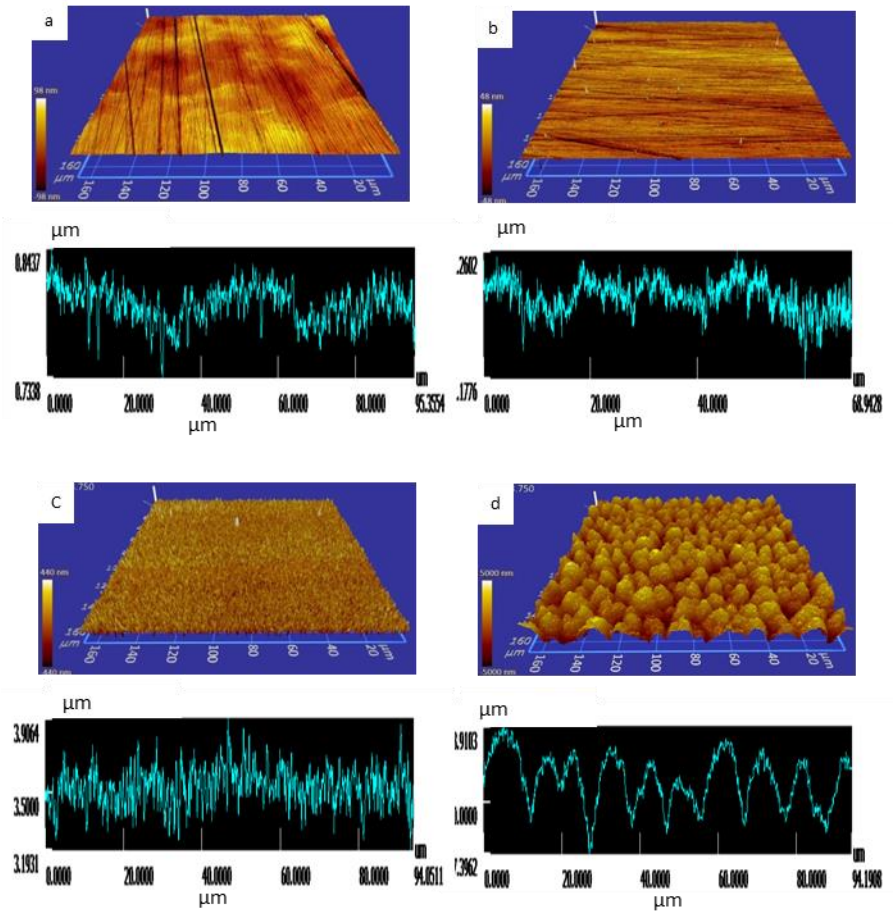

Fig.3. Wight Light Interferometer 2D and 3D profiler of the surfaces produced using laser: (a) control, (b) SS1, (c) SS2 and (d) SS3.

spaced, rounded surface features (Fig. 2, 3c). Surface produced using a laser speed of 1 mm/s demonstrated oval shaped, rounded topped surface features, pillow like structure (Fig. 2, 3d). It had the largest maximum peak height (7.57 µm) and valley depth values (6.70 µm).

The S_a, S_q and S_{pv} measurements were taken for all the surfaces (Fig. 4). S_a and S_q values demonstrated that SS3 demonstrated the greatest S_a, S_q and S_{pv} values (1.31, 1.60 and 11.80 µm). SS1 and SS2 demonstrated values similar to that of the control (0.02 µm / 0.04 µm; 0.09 µm / 0.11 µm; 0.02 µm / 0.02 µm respectively), however, they (SS1 and SS2) demonstrated greater S_{pv} values than the control (1.4 µm, 1.59 µm and 0.82 µm respectively). The smoothest laser treated surfaces is SS1 while the rougher on is SS3.

AFM was used to determine the nano-features of the laser etched surfaces (Fig. 5). The results demonstrated that the nano-features for the SS1 and SS2 surfaces were more rounded in shape with sharp peaks like spikes than for the SS3 surfaces. Moreover, the surface features for the SS3 surface in terms of the peak width and height and valley depth and width were of the largest sizes even at the nanoscale (Table 3).

Table 2 Maximum width and height of the surface features

	Max peak width (µm)	Max peak height (µm)	Max valley width (µm)	Max valley depth (µm)
Control	3.61	0.06	1.24	0.09
SS1	1.98	0.06	1.73	0.12
SS2	3.31	0.52	2.42	0.51
SS3	17.90	7.57	17.90	6.70

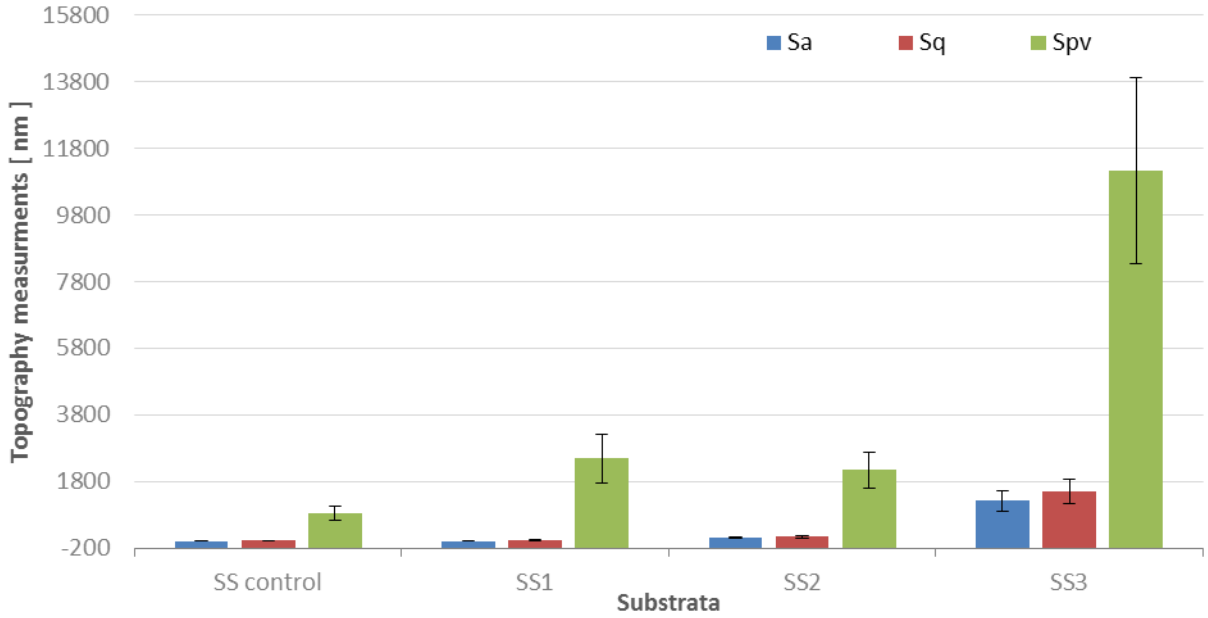

Fig. 4 Surface topography values for the laser etched stainless steel surfaces

Table 3 Average width and height of the surface features using AFM profiler

	Average peak width (µm)	Average peak height (µm)	Average valley width (µm)	Average valley depth (µm)
Control	0.09 (0.05)	0.002 (0.002)	0.09 (0.05)	0.002 (0.002)
SS1	0.08 (0.04)	0.01 (0.01)	0.11 (0.07)	0.01 (0.01)
SS2	0.34 (0.20)	0.08 (0.06)	0.27 (0.20)	0.10 (0.07)
SS3	0.46 (0.30)	0.15 (0.14)	0.33 (0.13)	0.18 (0.15)

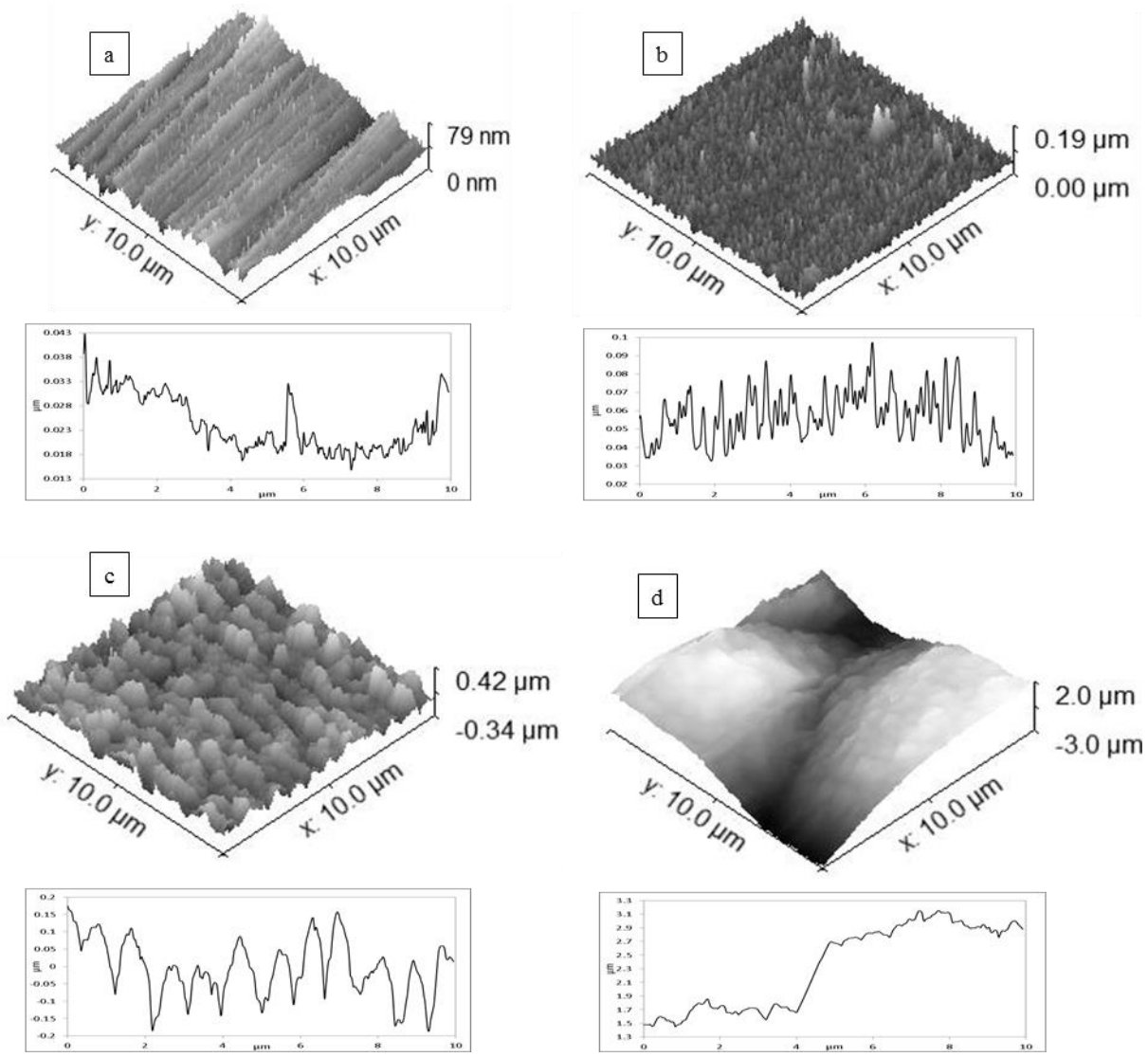

Fig. 5 AFM images of the different surface nano features: (a) control, (b) SS1, (c) SS2, (d) SS3,

The water contact angle of the laser treated surfaces was measured (Fig. 6). It is clear that the SS1 was of low CA and SS3 was of higher one.

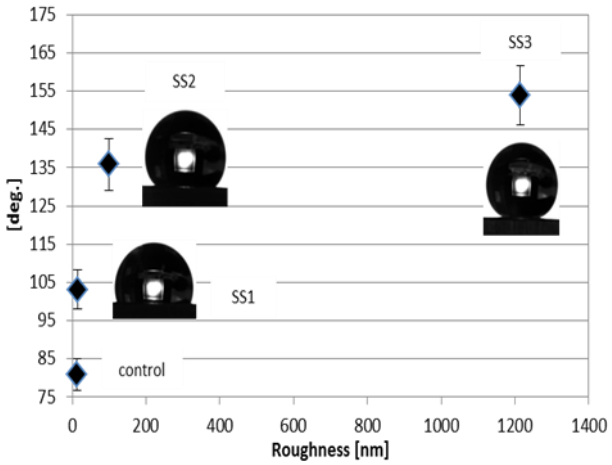

Fig. 6 Contact angle measurements of laser treated surfaces.

Energy dispersive X-Ray data (Table 4) demonstrated that the overall composition of the surfaces following laser treatment were iron, with oxygen, nitrogen, chromium and nickel with some fluorine. Interestingly the atomic fluorine level for SS3 was higher than that obtained for SS1 and SS2. The O:SS ratios from EDX were 0, 0.04 and 0.49, for SS1, SS2 and SS3 respectively. SS3 was of higher oxide ratio. The higher oxide layer may therefore increase the adsorption of the FAS. As the O:SS ratio for SS1 was the lowest recorded, there is likely to be only a smaller amount FAS adsorption observed.

3.2 Microbiology

The attachment, adhesion and retention of the bacteria were determined using three different microbiological assays (spray with wash, spray and retention). The SEM image of the E.coli bacteria attached on all surfaces following all assays was demonstrated (Fig.7). A small number of

Table 4 Atomic percentages of elements in the surfaces detected by EDX.

Element	**Element Amount (At %)**			
	control	SS1	SS2	SS3
Fe	64.86 (0.08)	63.25(0.53)	59.45 (0.9)	40.18 (1.50)
Cr	17.28 (0.10)	16.90 (0.10)	16.00 (0.35)	11.52 (0.40)
Ni	9.38 (0.14)	9.15 (0.10)	8.39 (0.28)	5.34 (0.36)
Mo	1.41 (0.13)	1.42 (0.03)	1.40 (0.04)	0.82 (0.08)
O	0	0	3.21 (0.87)	28.44 (0.94)
N	3.96 (0.07)	5.86 (1.83)	5.81 (0.59)	5.55 (0.50)
C	1.91 (0.00)	2.93 (0.70)	3.40 (0.26)	4.00(0.31)
F	0.57(0.08)	0.87 (0.03)	1.43 (0.58)	3.20 (0.92)
Si	0.61 (0.21)	0.60 (0.02)	0.91 (0.12)	0.92 (0.06)
O:SS(F+Ni+Cr+Mo)		0	0.04	0.49
F:SS		0.01	0.02	0.06

bacteria were observed on all the surfaces following all the assays (Fig. 8). It was clear that, following the adhesion (spray) assays, the greatest number of cells was retained on the control (234), then SS1 (53) followed by SS2(41), whereas, the lowest numbers were retained on SS3 (21). Following the attachment (spray with wash) assay that the greatest numbers of bacteria were retained on the control surface (31), followed by the SS2 (10) with the least retained on SS3 (7). Following the retention assay, the greatest numbers of cells were retained on the control surface (78) followed by the SS1 (32) with no difference between SS2 and SS3. Overall, it can be said that SS3 was the best surfaces with less number of bacteria retention comparing with other surfaces.

4. Discussion

4.1 Laser Surface Texture

In the current work, ps laser ablation was used to develop different macro / micro structures on 316L stainless steel surfaces, through processing at different fluence, hatch distances, scanning time and scanning speeds. The change of surface morphology and roughness of the laser textured surfaces is attributed to the change in laser scanning parameters and physiothermal properties of the used substrate. Using different hatch distances and scanning speeds affected the overlapping in the direction of scanning direction and in the direction perpendicular to scanning direction. Using scanning speeds of 1, 100 and 1000, the overlapping in the scanning direction was, respectively, 99.99%, 99.2% and 92.2%. However, the overlapping in the direction perpendicular to scanning direction was 60%, 36% and 92% using, respectively, 50 µm, 80 µm and 10 µm hatch distances. Taking all these into account, it is clear that heat accumulation effect was the reason behind inducing different macro/micro/nano structures. In case of rims structure (SS1), the overlapping in both directions was low comparing with other surfaces resulting in a low fluence irradiating a surface which in turns melting the surface took place and formed a rim structure and low roughness. In case of SS2, the overlapping in both directions was increased comparing to SS1. It was clear that the main mechanism of structuring was ripples or Laser Induced Periodic Surface Structure (LIPSS). In case of pillow like structures (SS3), there was very large overlapping in both directions resulting in a considerable amount of laser intensity irradiating a specific small surface area. The local overheating of the material may occur and, in addition to material ablation, enhanced material melting can potentially take place. The structure of the circular forms covering the surface was a result of sintering of ablated materials together forming these particles [23].

Taking into account the effect of laser parameters, it was found that the surface generated using very low speed and / or small hatch distance (SS3) were hydrophobic with water contact angle > 150˚. The surfaces demonstrated hierarchical structures with increased roughness. This may be a result of the surface topographies resulting in increased air being trapped between the features thus increasing the hydrophobicity [24, 25]. However, it has been found that with increasing the hatch distances and / or increasing scanning speed, the hydrophobicity was decreased. This might be attributed to decreasing the overlapping with increasing the hatch distances and increasing the scanning speed resulted in the roughness decreasing [26]. In this work, the Cassie model was considered as the droplet of water did not wet the surface completely [20].

4.2 Microbiology

An understanding of how surface properties affect the attachment, adhesion and retention of bacteria may assist in designing or modifying the surfaces to discourage the bacteria biofouling [27]. The retention of bacteria on the surfaces depends on several factors such as surface Topography, chemistry, surface wettability and surface free energy. The several range of surfaces roughness, produced in this work, showed that bacterial attachment, adhesion and retention was lower for the laser treated surfaces compared with the untreated surface. Overall, SS3 performed the best

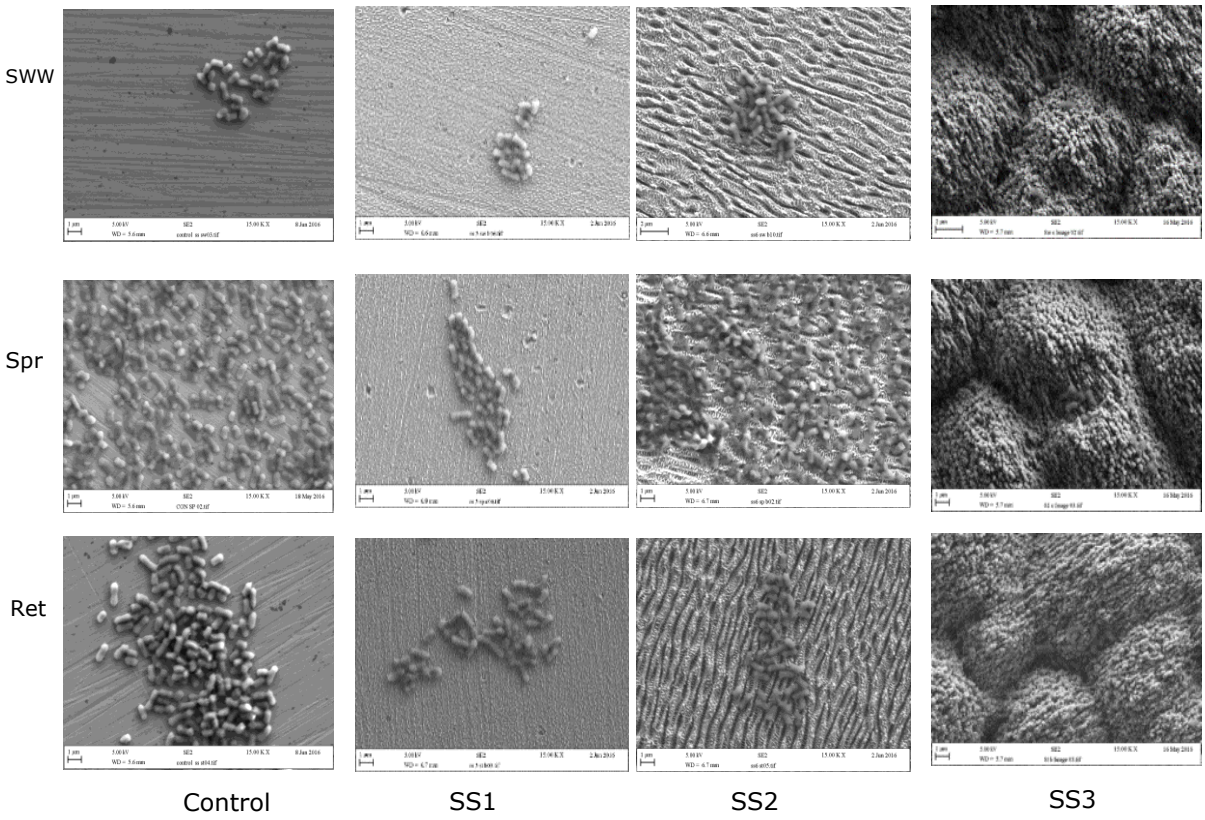

Fig. 7 Distribution of the bacteria across the surfaces following the three assays Spray = Spr, SWW = spray with wash and Ret = retention.

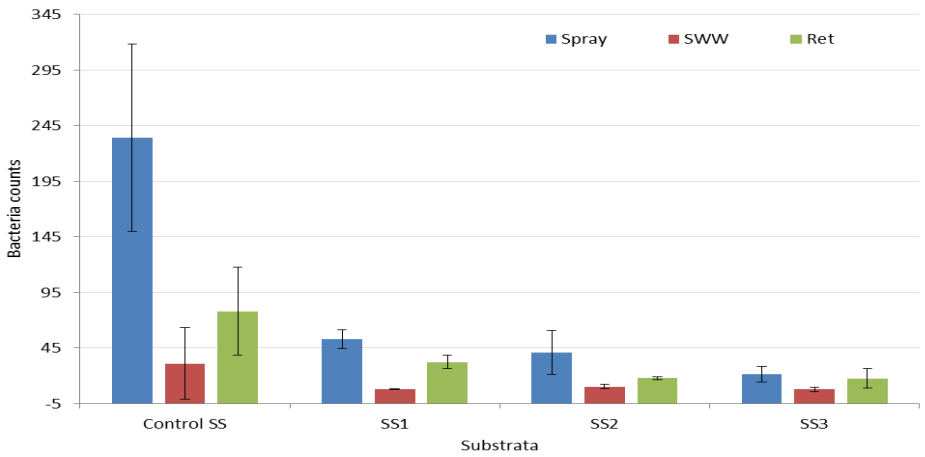

Fig. 8 Average number of *E.coli* retained on stainless steel surfaces following three different assays, spray, spray with wash and retention.

in all three assays and had the widest peaks and values and the most hydrophobic. The surfaces that retained the greatest number of bacteria demonstrated the lowest S_a, S_q, S_{pv} values and hydrophobicity. Thus the results suggest that surface superhydrophobic properties need to be used in conjunction with defined specific surface topography in order to reduce bacteria attachment adhesion and retention.

5. Conclusions

In this work, antiadhesive property of three self-organized structures induced on stainless steel substrate using picosecond laser irradiating was investigated. It was proved that the surface roughness and surface wettability affected the amount of bacteria attachment. The results showed that the laser processing significantly reduced the adhesion of bacteria by producing a superhydrophobic surface with a defined topography thus reducing the area of contact between bacteria and the surface. One surface was demonstrated to be the best antiadhesive surface which was of hierarchal superhydrophobic, had the greatest S_a and S_{pv} value, and the greatest peak and valley widths with nanoparticles covered the macro and micro features.

Acknowledgments

The authors would like to thank Iraqi Ministry of Higher Education and Scientific Research (MOHESR) for the financial support of Fatema Rajab's PhD research.

References

[1]. Whitehead K and Verran J, *The effect of substratum properties on the survival of attached microorganisms on inert surfaces*, in *Marine and industrial biofouling*. Springer; 2009. p. 13-33.

[2]. Whitehead K A and Verran J. The effect of surface topography on the retention of microorganisms. Food and Bioproducts Processing 2006; 84: 253-259.

[3]. Tetlow L A, Lynch S, and Whitehead K A. The effect of surface properties on bacterial retention: A study utilising stainless steel and TiN/25.65 at.% Ag substrata. Food and Bioproducts Processing 2017; 102: 332-339.

[4]. Dantas L C d M, Silva-Neto J P d, Dantas T S, Naves L Z, das Neves F D, and da Mota A S. Bacterial Adhesion and Surface Roughness for Different Clinical Techniques for Acrylic Polymethyl Methacrylate. International Journal of Dentistry 2016; 2016:

[5]. Wang H, Feng H, Liang W, Luo Y, and Malyarchuk V. Effect of surface roughness on retention and removal of Escherichia coli O157: H7 on surfaces of selected fruits. Journal of food science 2009; 74:

[6]. Whitehead K, Benson P, and Verran J. The detection of food soils on stainless steel using energy dispersive X-ray and Fourier transform infrared spectroscopy. Biofouling 2011; 27: 907-917.

[7]. Whitehead K A, Colligon J, and Verran J. Retention of microbial cells in substratum surface features of micrometer and sub-micrometer dimensions. Colloids and Surfaces B: Biointerfaces 2005; 41: 129-138.

[8]. Milledge J J. The cleanability of stainless steel used as a food contact surface: an updated short review. Food Science and Technology Journal 2010; 24: 27-28.

[9]. Fadeeva E, Truong V K, Stiesch M, Chichkov B N, Crawford R J, Wang J, and Ivanova E P. Bacterial retention on superhydrophobic titanium surfaces fabricated by femtosecond laser ablation. Langmuir 2011; 27: 3012-3019.

[10]. Dou X-Q, Zhang D, Feng C, and Jiang L. Bioinspired hierarchical surface structures with tunable wettability for regulating bacteria adhesion. ACS nano 2015; 9: 10664-10672.

[11]. Privett B J, Youn J, Hong S A, Lee J, Han J, Shin J H, and Schoenfisch M H. Antibacterial fluorinated silica colloid superhydrophobic surfaces. Langmuir 2011; 27: 9597-9601.

[12]. Cunha A, Elie A-M, Plawinski L, Serro A P, do Rego A M B, Almeida A, Urdaci M C, Durrieu M-C, and Vilar R. Femtosecond laser surface texturing of titanium as a method to reduce the adhesion of Staphylococcus aureus and biofilm formation. Applied Surface Science 2016; 360: 485-493.

[13]. Yan Y Y, Gao N, and Barthlott W. Mimicking natural superhydrophobic surfaces and grasping the wetting process: a review on recent progress in preparing superhydrophobic surfaces. Advances in colloid and interface science 2011; 169: 80-105.

[14]. Crick C R, Ismail S, Pratten J, and Parkin I P. An investigation into bacterial attachment to an elastomeric superhydrophobic surface prepared via aerosol assisted deposition. Thin Solid Films 2011; 519: 3722-3727.

[15]. Gold J, Nilsson B, and Kasemo B. Microfabricated metal and oxide fibers for biological applications. Journal of Vacuum Science & Technology A 1995; 13: 2638-2643.

[16]. Chou S Y, Krauss P R, and Renstrom P J. Imprint of sub‐25 nm vias and trenches in polymers. Appl Phys Lett 1995; 67: 3114-3116.

[17]. Green A M, Jansen J A, Van der Waerden J, and Von Recum A F. Fibroblast response to microtextured silicone surfaces: texture orientation into or out of the surface. Journal of biomedical materials research 1994; 28: 647-653.

[18]. Voisey K, Scotchford C, Martin L, and Gill H. Effect of Q-switched laser surface texturing of titanium on osteoblast cell response. Physics Procedia 2014; 56: 1126-1135.

[19]. Cunha A, Serro A P, Oliveira V, Almeida A, Vilar R, and Durrieu M-C. Wetting behaviour of femtosecond laser textured Ti–6Al–4V surfaces. Applied Surface Science 2013; 265: 688-696.

[20]. Long J, Pan L, Fan P, Gong D, Jiang D, Zhang H, Li L, and Zhong M. Cassie-State Stability of Metallic Superhydrophobic Surfaces with Various Micro/Nanostructures Produced by a Femtosecond Laser. Langmuir 2016; 32: 1065-1072.

[21]. Long J, Zhong M, Fan P, Gong D, and Zhang H. Wettability conversion of ultrafast laser structured copper surface. J Laser Appl 2015; 27: S29107.

[22]. Long J, Fan P, Gong D, Jiang D, Zhang H, Li L, and Zhong M. Superhydrophobic Surfaces Fabricated by Femtosecond Laser with Tunable Water Adhesion From Lotus Leaf to Rose Petal. ACS applied materials & interfaces 2015;

[23]. Li Y, Cui Z, Wang W, Lin C, and Tsai H-L. Formation of linked nanostructure-textured mound-shaped microstructures on stainless steel surface via femtosecond laser ablation. Applied Surface Science 2015; 324: 775-783.

[24]. Moradi S, Kamal S, Englezos P, and Hatzikiriakos S G. Femtosecond laser irradiation of metallic surfaces: effects of laser parameters on superhydrophobicity. Nanotechnology 2013; 24: 415302.

[25]. Long J, Fan P, Zhong M, Zhang H, Xie Y, and Lin C. Superhydrophobic and colorful copper surfaces fabricated by picosecond laser induced periodic nanostructures. Applied Surface Science 2014; 311: 461-467.

[26]. Lehr J and Kietzig A-M. Production of homogenous micro-structures by femtosecond laser micro-machining. Opt Laser Eng 2014; 57: 121-129.

[27]. Flint S, Brooks J, and Bremer P. Properties of the stainless steel substrate, influencing the adhesion of thermo-resistant streptococci. Journal of Food Engineering 2000; 43: 235-242.